Broadband energy harvesting via magnetic coupling between two movable magnets*

Fan Kang-Qi(樊康旗)†, Xu Chun-Hui(徐春辉), Wang Wei-Dong(王卫东), and Fang Yang(方 阳)

School of Electronical & Mechanical Engineering, Xidian University, Xi'an 710071, *China*

(Received 1 November 2013; revised manuscript received 23 December 2013; published online 10 June 2014)

Harvesting energy from ambient mechanical vibrations by the piezoelectric effect has been proposed for powering microelectromechanical systems and replacing batteries that have a finite life span. A conventional piezoelectric energy harvester (PEH) is usually designed as a linear resonator, and suffers from a narrow operating bandwidth. To achieve broadband energy harvesting, in this paper we introduce a concept and describe the realization of a novel nonlinear PEH. The proposed PEH consists of a primary piezoelectric cantilever beam coupled to an auxiliary piezoelectric cantilever beam through two movable magnets. For predicting the nonlinear response from the proposed PEH, lumped parameter models are established for the two beams. Both simulation and experiment reveal that for the primary beam, the introduction of magnetic coupling can expand the operating bandwidth as well as improve the output voltage. For the auxiliary beam, the magnitude of the output voltage is slightly reduced, but additional output is observed at off-resonance frequencies. Therefore, broadband energy harvesting can be obtained from both the primary beam and the auxiliary beam.

Keywords: piezoelectric conversion, mechanical vibration, magnetic coupling, energy harvesting

PACS: 45.20.dg, 46.70.De, 68.35.Gy **DOI:** 10.1088/1674-1056/23/8/084501

1. Introduction

Microelectromechanical systems (MEMS) and the relevant physical mechanisms have attracted significant attention over the past few years due to their potential applications in many industries.[1–7] Currently, these systems are being powered and sustained by batteries that fail to keep pace with the demands of such systems, especially in terms of energy density.[8] Moreover, batteries require frequent replacement/recharge, which is prohibitively expensive and cumbersome for a large quantity or in a remote area.

Harvesting energy from ambient mechanical vibrations has been considered as a promising solution to this issue.[9–13] The ultimate aim is to implement self-powered systems.[11] Mechanical vibration can be converted into electrical energy as a power supply via electrostatic,[14] electromagnetic,[15] or piezoelectric transductions.[16–18] The piezoelectric transduction outperforms the others because of its high energy density, appropriate voltage and current outputs, strong electromechanical coupling, simple structure, and good compatibility with MEMS.[19–21] A conventional piezoelectric energy harvester (PEH) is generally designed as a single degree-of-freedom (DOF) linear resonator. In order to harvest energy efficiently, the resonant frequency of the PEH must match the frequency of the vibration source. However, this requirement cannot always be guaranteed since the frequencies of the naturally occurring vibration sources usually vary in a certain range. With a slight drift from the resonance, the efficiency of a conventional linear PEH will decrease dramatically.

In order to widen the operating bandwidth, and thus improve the performance of a PEH, several strategies have been proposed in recent years. The first strategy is to tune the resonant frequency of a PEH by applying mechanical preload,[16] using magnetic forces,[22] or piezoelectric actuators.[23] However, the complexity and power consumption of automatic tuning schemes may completely offset any improvement achieved in the performance of a PEH.[24,25] Multimodal energy harvesting is another strategy widely pursued for broadband purposes. This strategy can be utilized by integrating a piezoelectric cantilever array in one harvester,[26] or by exploiting two DOF PEH configurations.[27,28] In general, the purpose of developing a multimodal PEH is to achieve close resonances, but most of the multimodal energy harvesting schemes can only provide a discrete effective bandwidth.[28] In addition, multimodal energy harvesting increases the volume, and then reduces the energy density of a PEH.

In very recent years, magnetic interaction has been frequently reported for broadband energy harvesting. Cotton *et al.*[9] developed a piezoelectric inverted pendulum with bistable state to enhance energy harvesting from stochastic vibrations. Lin *et al.*[24] and Ferrari *et al.*[29] proposed simplified models to study the effect of nonlinear magnetic force on the performance of a PEH. They found that the off-resonance response of a PEH can be substantially improved by magnetic coupling. The dynamic responses of nonlinear PEHs

*Project supported by the National Natural Science Foundation of China (Grant No. 51205302) and the Fundamental Research Funds for the Central Universities, China (Grant No. K5051304011).

†Corresponding author. E-mail: kangqifan@gmail.com

© 2014 Chinese Physical Society and IOP Publishing Ltd

with different magnet separation under various excitation levels have also be analytically modeled and experimentally validated by some researchers.[12,30,31] Audò *et al.*[32] designed an antiphase bistable PEH that is realized by introducing the repulsive magnetic force between two parallel-aligned cantilever beams. Audò *et al.*[33] also presented a two-dimensional PEH by establishing magnetic coupling between two beams vibrating in the orthogonal directions. However, at low-level excitation, the aforementioned nonlinear PEHs fail to acquire enough kinetic energy to jump between two bistable states, and thus display no obvious superiority to the linear PEH. To address this issue, Tang and Yang[11] proposed a nonlinear PEH with a magnetic oscillator that covers a useful range of 23 Hz–29 Hz when excited at 2 m/s^2 (RMS value). The improved performance of this PEH is attributed to the magnetic oscillator that transfers part of its vibration energy to the PEH via magnetic interaction. Wu *et al.*[34] developed a nonlinear two-DOF PEH that comprises a main beam and an enclosed secondary beam attached to the main beam. The nonlinear behavior of this PEH is produced by the magnetic interaction between the two beams. Su *et al.*[35] realized a bistable PEH by employing the magnetic coupling between two beams that vibrate along the polarization direction of the magnets, and demonstrated its wider operating frequency than the linear PEH. But the cause of the improved performance was not provided. Zhu and Zu[36] reported a buckled-beam PEH and found that the PEH performance can be improved by exerting a magnetic force on the midpoint of the beam. Piezoelectric materials can also be combined with piezomagnetic materials to harvest the ambient magnetic energy or the magnetic energy converted from the mechanical vibration.[37,38]

In the present paper, we introduce a concept and describe the realization of a novel nonlinear PEH to scavenge energy from broadband mechanical vibrations. The proposed PEH is structured by two piezoelectric cantilever beams that are coupled together by two movable magnets. The primary beam is enclosed in the auxiliary beam to form a compact configuration. The two beams vibrate perpendicularly to the polarization direction of the magnets. Lumped parameter models are established to predict the nonlinear response from the proposed PEH. Experiments are also conducted to validate the theoretical predictions. It will be shown that the proposed PEH can achieve broadband energy harvesting by exploiting the magnetic coupling between the two movable magnets.

2. Formation of the proposed PEH

2.1. Linear PEH

A conventional PEH is generally composed of a piezoelectric cantilever beam. This typical linear PEH is usually fabricated from two piezoelectric layers and a metal shim, i.e., a triple-layer piezoelectric cantilever beam as shown in Fig. 1(a). The two piezoelectric layers can be electrically connected in series or parallel, and the latter case is considered in this work since it can produce the highest power under lower frequencies than the former case.[39] This triple-layer piezoelectric cantilever beam is designed to operate in the transverse mode (3-1 mode), which is the general case for the bending deformation as shown in Fig. 2. When the proof mass affixed at the free end of the piezoelectric cantilever beam is forced to vibrate by the ambient mechanical vibration, an applied mechanical stress T_1 along axis-1 is produced in the piezoelectric layer, which induces an electric displacement D_3 along axis-3. In the meantime, the applied electrical field E_3 along axis-3 affects the mechanical strain S_1 along axis-1. The coupling equations for 3-1 mode are

$$D_3 = d_{31}T_1 + \varepsilon_{33}E_3, \tag{1}$$

$$S_1 = s_{11}T_1 + d_{31}E_3, \tag{2}$$

where s_{11}, ε_{33}, and d_{31} are the compliance, permittivity, and piezoelectric coefficient of the piezoelectric material, respectively.

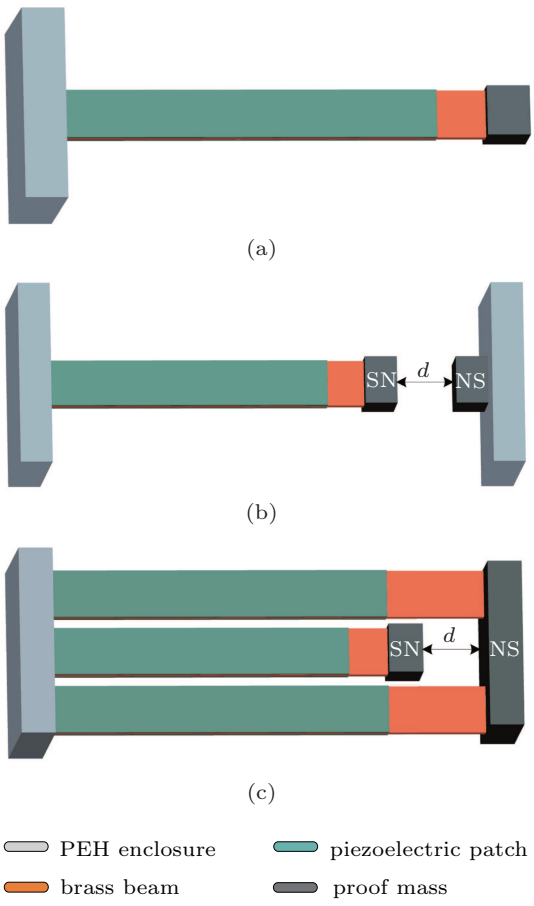


Fig. 1. (color online) Schematic diagram of different PEHs. (a) Linear PEH; (b) conventional nonlinear PEH; and (c) proposed PEH.

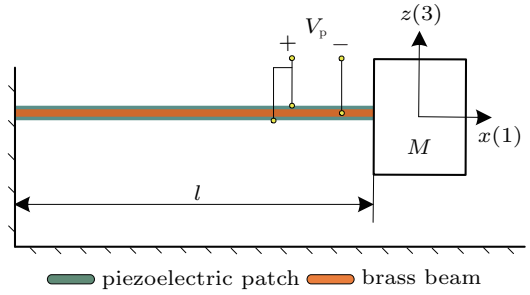


Fig. 2. (color online) Schematic diagram of a linear PEH.

The linear PEH is often modeled as a mass + spring + damper + piezo structure.[13,40–42] The governing equations of the linear PEH can be described by

$$M\ddot{z}(t)+\eta\dot{z}(t)+Kz(t)+\Theta V_{\mathrm{P}}(t)=F(t), \tag{3}$$

$$-\Theta\dot{z}(t)+C_{\mathrm{P}}\dot{V}_{\mathrm{P}}(t)=-I(t). \tag{4}$$

This is the lumped parameter model of the linear PEH, where $z(t)$ is the displacement of the proof mass M, η is the mechanical damping coefficient, K is the effective stiffness, Θ is the effective piezoelectric coefficient, C_{P} is the clamped capacitance of the piezoelectric layers, $V_{\mathrm{P}}(t)$ and $I(t)$ are the voltage and current outputs from the PEH respectively, and $F(t)$ is the applied force originating from the mechanical vibration of the base.

The linear PEH has only one resonant frequency, which must match the frequency of the external vibration source so as to generate sufficient power. With a slight drift from the resonance, the harvested energy will reduce markedly. However, many naturally occurring vibration sources do not have a fixed vibration frequency, and vibrate over a certain frequency range. Therefore, the frequency matching between the linear PEH and the vibration source cannot always be guaranteed. This indicates that only a small amount of the available energy can be harvested from the vibration sources. To tackle this issue, several strategies have been proposed. The most promising one is to incorporate magnets into the linear PEH to generate a nonlinear PEH.[9,12,24,25,29]

2.2. Conventional nonlinear PEH

The conventional nonlinear PEH is usually formed by adding one permanent magnet to the free end of the piezoelectric cantilever beam, and fixing another magnet at the enclosure of the PEH, as shown in Fig. 1(b). The potential energy of this system can be expressed as follows:[9,25,31]

$$U(z)=\frac{1}{2}Kz(t)^2+\frac{\mu_0 m_1 m_2}{2\pi}\left[z(t)^2+d^2\right]^{-3/2}, \tag{5}$$

where μ_0 is the permeability constant, m_1 and m_2 are the effective magnetic moments of the two magnets, and d is the distance between the two magnets. The first term on the right-hand side of Eq. (5) comes from the bending of the beam, whereas the second term results from the interaction between the two magnets.

Figure 3 shows the curves of the potential energy $U(z)$ for different values of separation d when $m_1=m_2=0.044$ A·m^2 and $K=100$ N·m^{-1}. For large distance d, the magnetic repulsive force is small, and then the system is monostable. In this case, the system behavior can be characterized by a quasilinear oscillator. By reducing the distance d, two potential energy minima or potential wells appear (shown in Fig. 3), resulting in the formation of a bistable configuration.

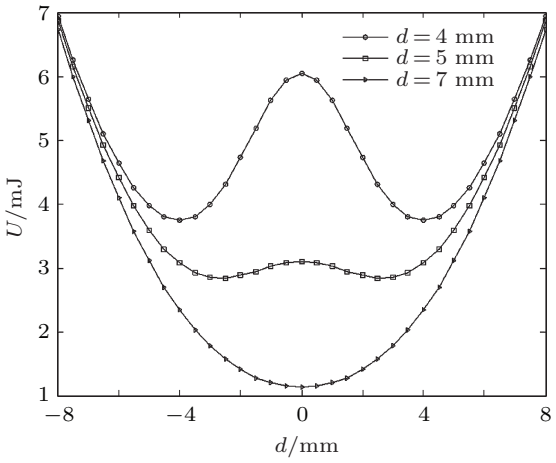


Fig. 3. Potential energy of the nonlinear PEH.

For the interaction between the two magnets, we assume that the magnetic force acts only in the vibration direction, and the magnetic force in the axial direction has a negligible effect on the beam vibration[12,24,25] (justification for this assumption is given below). In addition, we assume that the directions of the magnetic moments are always vertically aligned during the vibrations of the PEH. Based on these assumptions, the coupling force between the two magnets can be expressed as[9,25]

$$F_{\mathrm{m}}(t)=-\frac{3\mu_0 m_1 m_2 z(t)}{2\pi}\left[z(t)^2+d^2\right]^{-5/2}. \tag{6}$$

Adding $F_{\mathrm{m}}(t)$ to the left-hand side of Eq. (3) yields the governing equations of the nonlinear PEH coupled with a fixed magnet, i.e.,

$$M\ddot{z}(t)+\eta\dot{z}(t)+Kz(t)+\Theta V_{\mathrm{P}}(t)+F_{\mathrm{m}}(t)=F(t), \tag{7}$$

$$-\Theta\dot{z}(t)+C_{\mathrm{P}}\dot{V}_{\mathrm{P}}(t)=-I(t). \tag{8}$$

It has been shown that at sufficiently large excitation (e.g., 7 m/s in Ref. [24]), the conventional nonlinear PEH could implement broadband energy harvesting, provided that it can oscillate between the two potential wells resulting from the repulsive interaction between the two magnets.[9,25] However, for low-level excitation, the oscillation of the piezoelectric cantilever beam may be exclusively confined within one potential well and the system behavior could be characterized once again by a quasilinear oscillation around the minimum of

the confining well.[9] In this case, no obvious superiority to the linear PEH can be observed. In fact, a systematic experimental study performed by Tang *et al.*[25] indicated that the optimal nonlinear configuration is near the monostable-to-bistable region.

2.3. The proposed PEH

We propose to replace the fixed magnet at the enclosure with a movable magnet. One approach to realizing this configuration is to add an auxiliary piezoelectric cantilever beam to the linear PEH and establish magnetic coupling between the primary beam and the auxiliary beam as shown in Fig. 1(c). The magnetic coupling force is then modified into

$$F_{\mathrm{m}}(t) = -\frac{3\mu_0 m_1 m_2}{2\pi}[z_1(t)-z_2(t)] \times \left\{[z_1(t)-z_2(t)]^2+d^2\right\}^{-5/2}, \quad (9)$$

where $z_1(t)$ and $z_2(t)$ represent the displacements of the primary beam and auxiliary beam, respectively.

Substituting Eq. (9) into Eq. (7), we can obtain the governing equations of the primary beam as

$$M_1\ddot{z}_1(t)+\eta_1\dot{z}_1(t)+K_1 z_1(t) + \Theta_1 V_{\mathrm{P1}}(t)+F_{\mathrm{m}}(t)=F_1(t), \quad (10)$$

$$-\Theta_1\dot{z}_1(t)+C_{\mathrm{P1}}\dot{V}_{\mathrm{P1}}(t)=-I_1(t). \quad (11)$$

Simiarly, the governing equations of the auxiliary beam can be described as

$$M_2\ddot{z}_2(t)+\eta_2\dot{z}_2(t)+K_2 z_2(t) + \Theta_2 V_{\mathrm{P2}}(t)-F_{\mathrm{m}}(t)=F_2(t), \quad (12)$$

$$-\Theta_2\dot{z}_2(t)+C_{\mathrm{P2}}\dot{V}_{\mathrm{P2}}(t)=-I_2(t), \quad (13)$$

where the subscripts 1 and 2 in the parameters denote the primary beam and auxiliary beam, respectively.

If the auxiliary beam is fixed ($z_2(t)\equiv 0$), the proposed PEH degrades to a conventional nonlinear PEH as shown in Fig. 1(b). If the magnetic coupling is also eliminated ($F_{\mathrm{m}}(t)\equiv 0$), the proposed PEH degrades further to a conventional linear PEH as shown in Fig. 1(a). The governing equations of the PEH with various configurations can be solved numerically to capture their dynamic responses. For simplicity, the conventional nonlinear PEH is referred to as nonlinear PEH hereafter.

Following other researchers' work,[12,24,25] we ignore the influence of axial magnetic force acting on the beams. For our design, the two magnets each have an effective magnetic moment of 0.0042 A·m^2 and a span of 5 mm. In this case, the maximum axial magnetic force F_{m} is 0.0169 N and drops quickly with the distance along the vibration direction. The resonant frequency f_{m} of a beam under an axial force F_{m} is given by[24]

$$f_{\mathrm{m}} = f\sqrt{1-\frac{4F_{\mathrm{m}}L^2}{\pi^2 EI}}, \quad (14)$$

where f is the resonant frequency without axial force, E is the Young modulus, L is the length of the beam, and I is the moment of inertia.[43] Inserting the appropriate values into Eq. (14) gives frequency shifts of 0.17% and 0.24% for the primary beam and auxiliary beam, respectively. Therefore, the axial magnetic force is not a significant factor for our design.

3. Experimental setup

Experimental studies have also been conducted to verify the theoretical predictions. The prototype of the proposed PEH as well as the experimental setup is shown in Fig. 4. The devised prototype comprises a primary brass beam and an auxiliary beam fabricated by two identical brass sub-beams, each of which is sandwiched between two piezoelectric patches (PZT-5H). Two permanent magnets, spanning approximately 5 mm in the horizontal direction, are attached at the free ends of the primary beam and auxiliary beam, respectively. The two magnets have the same dimension of 1.2 mm×6 mm×1 mm, and an effective magnetic moment of 0.0042 A·m^2. The devised prototype can be easily converted into a nonlinear PEH by fixing the movable magnet at the PEH enclosure, or reduced to a linear PEH by removing the magnets. The dimension of the proposed

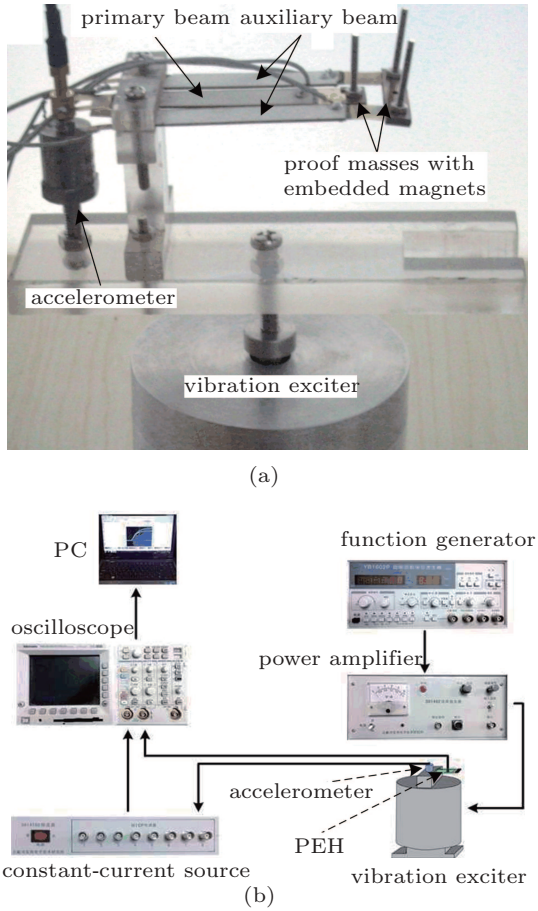


Fig. 4. (color online) (a) Prototype of the proposed PEH and (b) experimental setup.

PEH is given in Table 1. In the experiment, the PEH is excited by a vibration exciter that is driven by a harmonic signal. This signal is generated and regulated by a function generator and a power amplifier, respectively. The magnitude of excitation acceleration is controlled at 3 m/s^2, and the excitation frequency is manually swept from 15 Hz to 35 Hz. Measurements of the PEH response are performed by employing an accelerometer for measuring the base excitation, and an oscilloscope for recording the piezoelectric voltage.

Table 1. Dimension of the proposed PEH.

Primary beam	Brass beam	45 mm×10 mm×0.1 mm
	Piezoelectric patch	39 mm×10 mm×0.2 mm
Auxiliary beam	Brass beam	55 mm×10 mm×0.1 mm
	Piezoelectric patch	45 mm×10 mm×0.2 mm

In order to initiate the numerical simulation, we first need to obtain the system parameters from the experiment. This work is done by testing the primary beam and auxiliary beam separately using the model identification procedure presented by Tang and Yang.[11] In addition, since the two identical sub-beams of the auxiliary beam are fastened together via a proof mass, they respond to the applied excitation in the same way. Therefore, only one sub-beam is examined in the experiment. Hereafter, for the auxiliary beam, the results and discussion of experiment and simulation are based on the voltage obtained from this selected sub-beam. The identified system parameters are listed in Table 2.

Table 2. The identified system parameters.

Parameters	Primary beam	Auxiliary beam
M/g	1.30	3.96
η/N·s·m^{-1}	0.038	0.041
K/N·m^{-1}	31.4	61.1
Θ/m·N·V^{-1}	0.315	0.615
C/nF	28.7	31.1

4. Results and discussion

Figure 5 shows the open-circuit voltage responses of the primary beam from simulation and experiment for various configurations. For the linear configuration, the voltage at the resonant frequency (approximately 26 Hz) from simulation is 6.3 V. When the primary beam is coupled with a fixed magnet to form a nonlinear configuration, the frequency shifts toward the left and the resonant frequency reduces to 24.5 Hz. Moreover, the output voltage is found to increase significantly from both simulation and experiment. These changes result from the repulsive interaction between the primary beam and the fixed magnet. The repulsive interaction reduces the effective stiffness of the primary beam, and thus lowers the resonant frequency and enhance the beam deflection, resulting in an increase in the output voltage. If the primary beam is coupled with a movable magnet, although no obvious frequency shift is observed as compared with the nonlinear configuration, the maximum output voltage is increased, and the useful voltage output covers a broader frequency range. The improved performance of the primary beam with the proposed configuration could be attributed to the auxiliary beam that transfers part of its vibration energy to the primary beam via magnetic coupling.

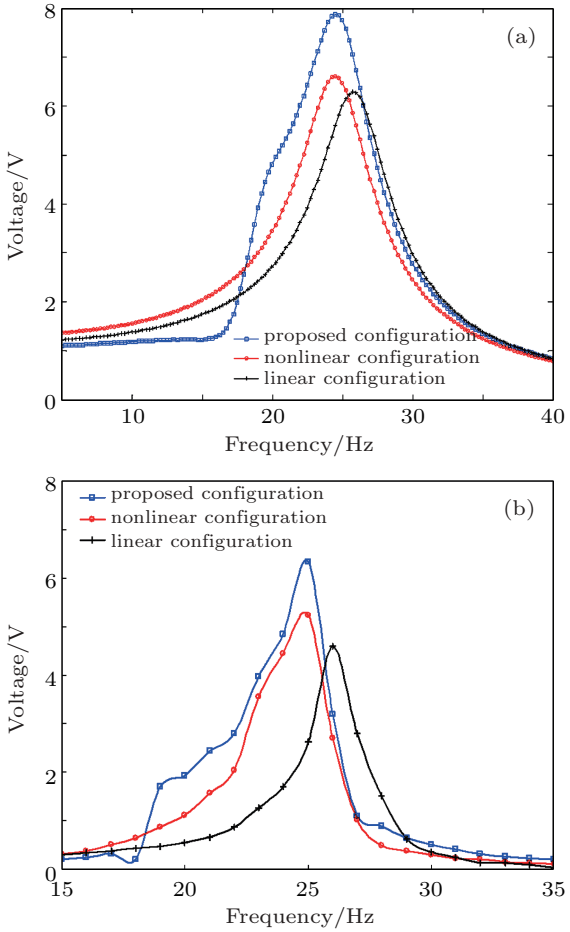


Fig. 5. (color online) Open-circuit voltage of primary beam from (a) simulation and (b) experiment.

Overall, the simulation predicts that the proposed configuration outperforms the linear and nonlinear configurations in the sense of output magnitude and bandwidth. This finding can be validated by the experimental observations as shown in Fig. 5(b). However, for the three configurations, simulation generally predicts a larger output voltage than the experiment. The discrepancy between simulation and experiment may due to two factors. First, the experimental observation could be affected by the disturbance from the background noise that is ignored in the simulation. Second, the damping may change with the vibration frequency in experiment,[11] but a constant

damping is used in the simulation. For the magnetic coupling configurations, the discrepancy may also come from the assumption that the magnetic moments are vertically aligned during beam vibration. This assumption overstates the magnetic interaction when the rotations at the free end of the beam are no longer negligible. Nevertheless, the simulation and experiment reveal that the primary beam with the proposed configuration could provide a wider bandwidth as well as an increased output voltage.

For the auxiliary beam with a linear configuration, the voltage at the resonant frequency (approximately 20 Hz) from simulation is 6.6 V. When the auxiliary beam is coupled with a fixed magnet to form a nonlinear configuration, the frequency shifts toward the left and the increase in the output voltage can also be observed from both simulation and experiment. If the auxiliary beam is coupled with a movable magnet, simulation and experiment indicate that the output voltage slightly decreases near its resonant frequency (approximately 18.6 Hz) as compared with the linear and nonlinear configurations as shown in Fig. 6. This is owing to the energy transfer from the auxiliary beam to the primary beam via magnetic coupling. However, the auxiliary beam with the proposed configuration can still provide significant output in the vicinity of its resonant frequency. Moreover, on the right side of the resonant frequency (near the resonant frequency of the primary beam), there is an additional output obtained for the proposed configuration, which is not observed for the linear and nonlinear configurations. Similarly, the additional output is attributed to the magnetic coupling between the primary beam and the auxiliary beam.

The magnetic coupling between the primary beam and the auxiliary beam can be illustrated by the variation of the vibration amplitude with the excitation frequency, as shown in Fig. 7. From Figs. 5–7, three important features can be identified. (i) For the primary beam, the vibration amplitude and output voltage each reach a plateau if the excitation frequency is smaller than 18.6 Hz. (ii) The vibration amplitude and output voltage of the primary beam increase remarkably when the excitation frequency varies from the resonant frequency of the auxiliary beam (18.6 Hz) to the resonant frequency of the primary beam (24.5 Hz). (iii) For the auxiliary beam, the vibration amplitude and output voltage are enhanced apparently near the resonant frequency of the primary beam.

The first feature can be explained as follows. For the primary beam, the magnetic force and applied force exhibit opposite variation trends, as shown in Fig. 8(a). This indicates that the magnetic coupling counteracts part of the external excitation, causing a reduction in the vibration amplitude and output voltage. However, within this frequency range (smaller than 18.6 Hz), the magnetic force and applied force have the same variation trend for the auxiliary beam, as shown in Fig. 8(b). This means that the magnetic coupling reinforces the external excitation applied to the auxiliary beam, and then provides an improved output voltage that is almost identical to that of the nonlinear configuration, as shown in Fig. 6.

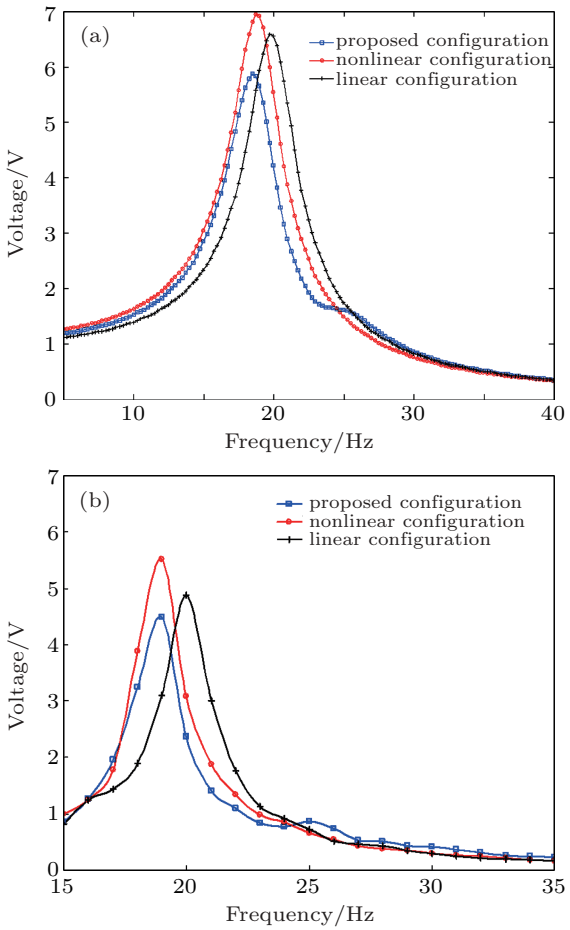


Fig. 6. (color online) Open-circuit voltage of auxiliary beam from (a) simulation and (b) experiment.

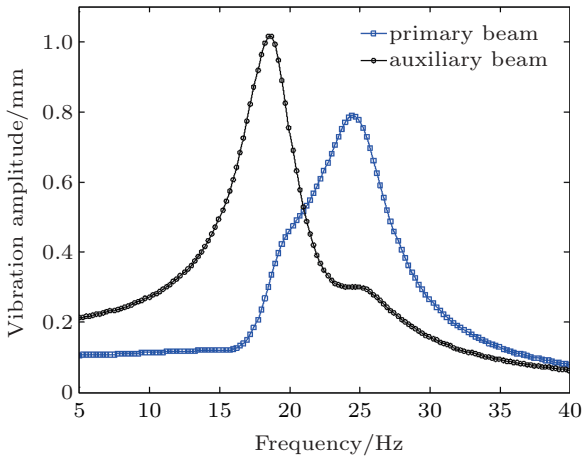


Fig. 7. (color online) Variations of vibration amplitude with excitation frequency.

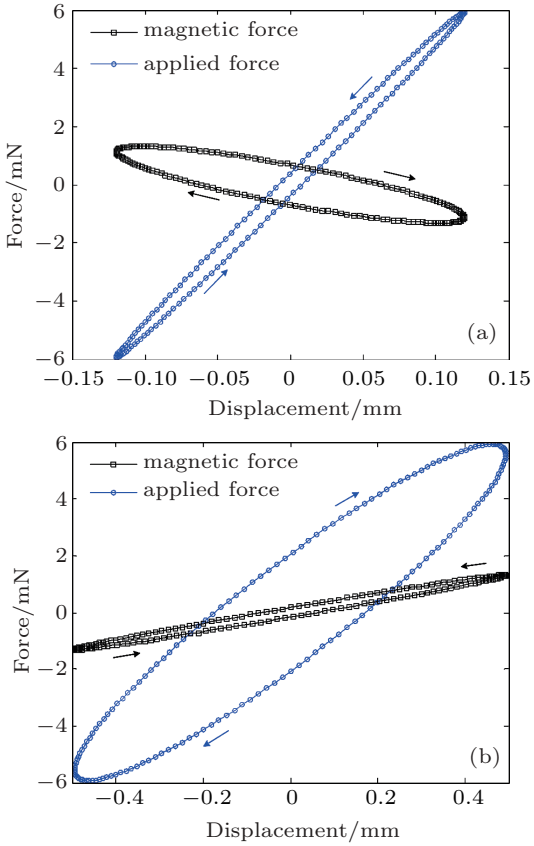


Fig. 8. (color online) Magnetic forces and applied forces at 15 Hz for (a) primary beam and (b) auxiliary beam.

The second feature can also be illustrated by the variations of the magnetic force and applied force with displacement, as shown in Fig. 9. When the excitation frequency varies from 18.6 Hz to 24.5 Hz, the magnetic coupling strengthens the external excitation for the primary beam, as shown in Fig. 9(a). However, for the auxiliary beam, the magnetic coupling offsets part of the external excitation, as shown in Fig. 9(b). Within this frequency range, the auxiliary beam transfers part of its energy to the primary beam, resulting in an increase in the output voltage of the primary beam.

The second and third features reveal that the output voltages from the primary beam and auxiliary beam can be improved simultaneously when the excitation frequency is near the resonant frequency of the primary beam. A survey on the magnetic force and applied force at an excitation frequency of 24.5 Hz (resonant frequency of the primary beam) shows that the two forces have the same variation trend in the most time of a vibration period for both the primary beam and auxiliary beam, as shown in Fig. 10. This finding indicates that the improved performance of the primary beam is not necessarily realized by the extra energy sourced from the auxiliary beam. The magnetic coupling could behave like an excitation source for both the primary beam and the auxiliary beam when the excitation frequency is near the resonant frequency of the primary beam.

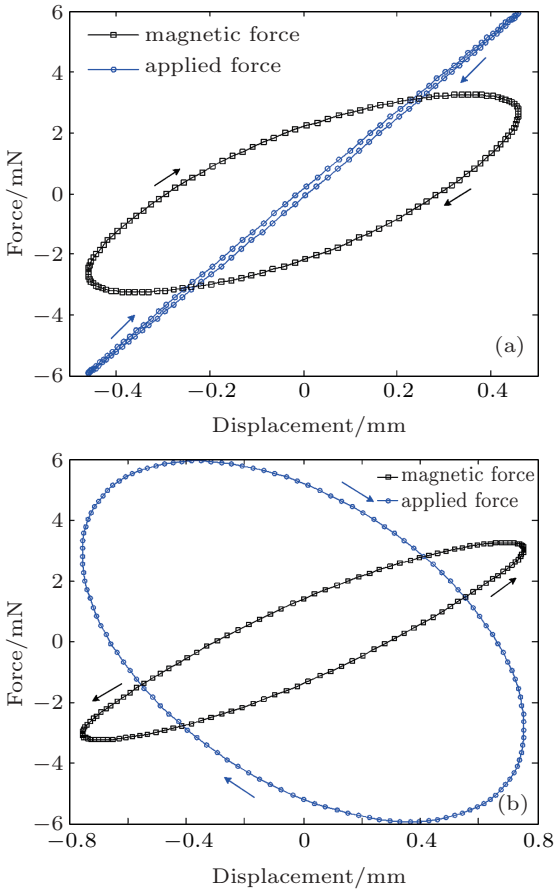


Fig. 9. (color online) Magnetic forces and applied forces at 20 Hz for (a) primary beam and (b) auxiliary beam.

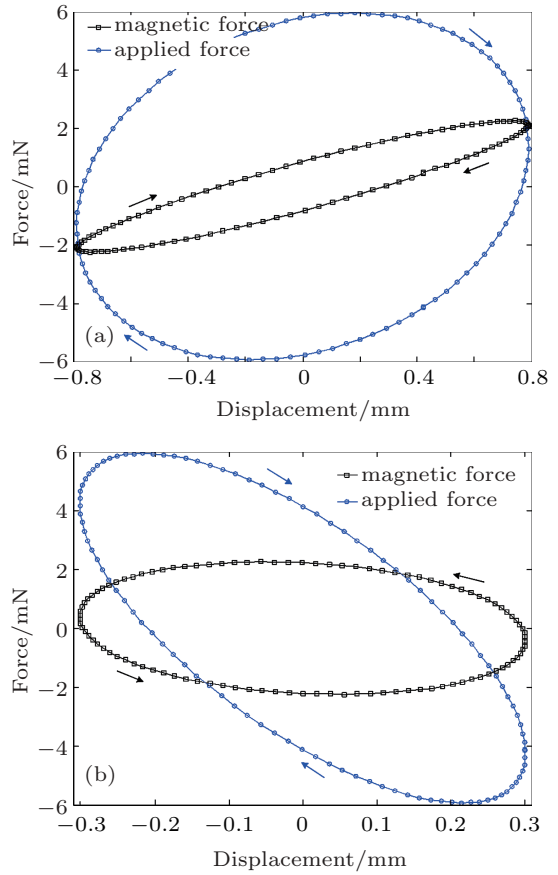


Fig. 10. (color online) Magnetic forces and applied forces at 24.5 Hz for (a) primary beam and (b) auxiliary beam.

A parameter study on $n = f_{n1}/f_{n2}$ is also conducted to provide a complete picture regarding the influence of magnetic coupling on the output of the proposed PEH, where f_{n1} and f_{n2} are, respectively, the resonant frequencies of the primary beam and the auxiliary beam. As the resonant frequency of the primary beam approaches to that of the auxiliary beam, the output voltage of the primary beam increases, but the bandwidth decreases, as shown in Fig. 11(a). For the auxiliary beam, the response trend is just the contrary, as shown in Fig. 11(b). This finding indicates that a certain tradeoff is required between the magnitude of output voltage and the bandwidth for the proposed PEH.

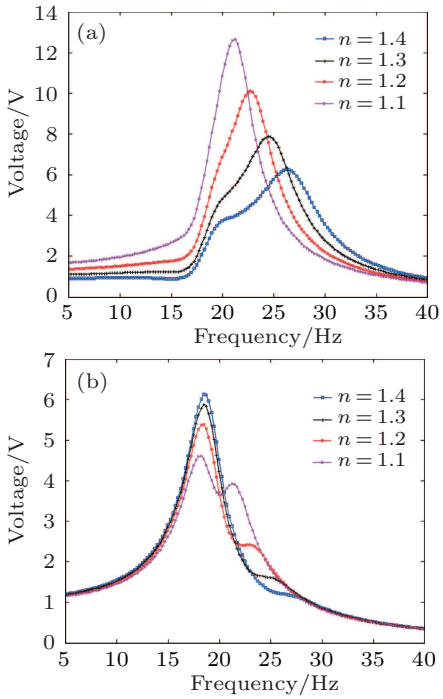


Fig. 11. (color online) Open-circuit voltages of (a) primary beam and (b) auxiliary beam for various configurations.

5. Conclusions

In this paper, we propose a novel nonlinear PEH that is realized via adding an auxiliary piezoelectric cantilever beam to the linear PEH and establishing magnetic coupling between the primary piezoelectric cantilever beam and the auxiliary piezoelectric cantilever beam. The lumped parameter model is established for predicting the dynamic response from the proposed PEH. Both simulation and experiment reveal that for the primary beam, the magnetic coupling can widen the operating bandwidth and in the meanwhile improve the output voltage. For the auxiliary beam, although the magnitude of output voltage is slightly reduced, an increase in the off-resonance output can be obtained. As a result, broadband energy harvesting can be achieved by both the primary beam and auxiliary beam. In addition, it is found that the tradeoff between the magnitude of output voltage and the bandwidth should be considered when using the proposed PEH configuration.

References

[1] Fan K Q, Jia J Y, Zhu Y M and Liu X Y 2007 *Acta Phys. Sin.* **56** 6345 (in Chinese)
[2] Yuse K, Monnier T, Petit L, Lefeuvre E, Richard C and Guyomar D 2008 *J. Intell. Mater. Syst. Struct.* **19** 387
[3] Yick J, Mukherjee B and Ghosal D 2008 *Comput. Netw.* **52** 2292
[4] Wang Z Q, Zhao Y P and Huang Z P 2010 *Int. J. Eng. Sci.* **48** 140
[5] Fan K Q, Jia J Y, Zhu Y M and Zhang X Y 2011 *Chin. Phys. B* **20** 043401
[6] Fan K Q, Wang W D, Zhu Y M and Zhang X Y 2011 *Sci. China: Phys. Mech. Astron.* **54** 1680
[7] Patricia M, Feng Q and Paul C 2011 *Int. J. Sens. Netw.* **10** 73
[8] Clair D S, Bibo A, Sennakesavababu V R, Daqaq M F and Li G 2010 *Appl. Phys. Lett.* **96** 144103
[9] Cottone F, Vocca H and Gammaitoni L 2009 *Phys. Rev. Lett.* **102** 080601
[10] Hu Y T, Wang J N, Yang F, Xue H, Hu H P and Wang J 2011 *IEEE T. Ultrason. Ferroelectr. Freq. Control* **58** 849
[11] Tang L H and Yang Y W 2012 *Appl. Phys. Lett.* **101** 094102
[12] Sun S and Cao S Q 2012 *Acta Phys. Sin.* **61** 210505 (in Chinese)
[13] Fan K Q, Ming Z F, Xu C H and Chao F B 2013 *Chin. Phys. B* **22** 104502
[14] Boisseau S, Despesse G and Sylvestre A 2010 *Smart Mater. Struct.* **19** 075015
[15] Zorlu Ö Topal E T and Külah H 2011 *IEEE Sens. J.* **11** 481
[16] Hu Y T, Xue H and Hu H P 2007 *Smart Mater. Struct.* **16** 1961
[17] He C, Chen H, Bai F, Fan Z, Sun L, Xu F, Wang J, Liu Y and Zhu K 2012 *J. Appl. Phys.* **112** 126102
[18] He C, Fu X, Xu F, Wang J, Zhu K, Du C and Liu Y 2012 *Chin. Phys. B* **21** 054207
[19] Zhu D B, Tudor M J and Beeby S P 2010 *Meas. Sci. Technol.* **21** 022001
[20] Renaud M, Karakaya K, Sterken T, Fiorini P, Van Hoof C and Puers R 2008 *Sens. Actuators A* **145** 380
[21] Shu Y C and Lien I C 2006 *Smart Mater. Struct.* **15** 1499
[22] Challa V R, Prasad M G and Fisher F T 2011 *Smart Mater. Struct.* **20** 025004
[23] Wischke M, Masur M, Goldschmidtboeing F and Woias P 2010 *J. Micromech. Microeng.* **20** 035025
[24] Lin J T, Lee B and Alphenaar B 2010 *Smart Mater. Struct.* **19** 045012
[25] Tang L H, Yang Y W and Soh C K 2012 *J. Intell. Mater. Syst. Struct.* **23** 1433
[26] Xue H, Hu Y T and Wang Q M 2008 *IEEE T. Ultrason. Ferroelectr. Freq. Control* **55** 2104
[27] Kim I H, Jung H J, Lee B M and Jang S J 2011 *Appl. Phys. Lett.* **98** 214102
[28] Wu H, Tang L H, Yang Y W and Soh C K 2012 *Jpn. J. Appl. Phys.* **51** 040211
[29] Ferrari M, Ferrari V, Guizzetti M, Andó B, Baglio S and Trigona C 2010 *Sens. Actuators A* **162** 425
[30] Stanton S C, McGehee C C and Mann B P 2010 *Physica D* **239** 640
[31] Audó B, Baglio S, Trigona C, Dumas N, Latorre L and Nouet P 2010 *J. Micromech. Microeng.* **20** 125020
[32] Andó B, Baglio S, Latorre L, Maiorca F, Nouet P and Trigona C 2012 *Procedia Engineering* **47** 1065
[33] Andó B, Baglio S, Maiorca F and Trigona C 2012 *Procedia Engineering* **47** 1061
[34] Wu H, Tang L H, Avvari P V, Yang Y W and Soh C K 2013 *Proceedings of SPIE Conference on Active and Passive Smart Structures and Integrated Systems* **8688** 86880B
[35] Su W J, Zu J and Zhu Y 2014 *J. Intell. Mater. Syst. Struct.* **25** 430
[36] Zhu Y and Zu J W 2013 *Appl. Phys. Lett.* **103** 041905
[37] Zhang C L, Yang J S and Chen W Q 2009 *Appl. Phys. Lett.* **95** 013511
[38] Zhang C L and Chen W Q 2010 *Appl. Phys. Lett.* **96** 123507
[39] Saadon S and Sidek O 2011 *Energ. Convers. Manage* **52** 500
[40] Lien I C, Shu Y C, Wu W J, Shiu S M and Lin H C 2010 *Smart Mater. Struct.* **19** 125009
[41] Wickenheiser A M, Reissman T, Wu W J and Garcia E 2010 *IEEEASME T. Mech.* **15** 400
[42] Yang Y W, Zhao L Y and Tang L H 2013 *Appl. Phys. Lett.* **102** 064105
[43] Roundy S and Wright P K 2004 *Smart Mater. Struct.* **13** 1131